Acta Poloniae Pharmaceutica – Drug Research, Vol. 79 No. 3 pp. 419-429, 2022
DOI: 10.32383/appdr/152437
Received 9 March 2022, Received in revised form 7 July 2022, Accepted 27 July 2022

ISSN 2353-5288
Polish Pharmaceutical Society

PHARMACOLOGY

THE EFFECTS OF RANOLAZINE ON COBALT CHLORIDE-INDUCED CHEMICAL HYPOXIA IN ENDOTHELIAL CELLS

EDIP G. CEKIC[1]*, GURKAN YIGITTURK[2], MELIKE O. ONAL[2], HULYA ELBE[2], NESRIN F. BASARAN[1] AND FERAL OZTURK[2]

[1]Department of Pharmacology, Faculty of Medicine, Mugla Sitki Kocman University, Turkey
[2]Department of Histology and Embryology, Faculty of Medicine, Mugla Sitki Kocman University, Turkey

Abstract: Ranolazine is beneficial when given as an adjunct to treatment in symptomatic angina pectoris. Therefore, it may be useful to evaluate the effect of ranolazine on cardiovascular endothelial cells in hypoxic conditions that may resemble decreased oxygen delivery during angina pectoris. In this study, chemical hypoxia caused by exposure of Human Umbilical Vein Endothelial Cells (HUVECs) to different concentrations of cobalt chloride ($CoCl_2$) (100 μM - 1000 μM) for 24 and 48 h was evaluated. In this chemical hypoxia model, HIF-1alpha and eNOS were measured semi-quantitatively by immunocytochemistry. Activation of the intracellular MAPK and PI3K pathways was evaluated by flow cytometry. During chemical hypoxia, HIF-1alpha was increased in a $CoCl_2$ concentration-dependent manner; however, eNOS did not change significantly. In the presence of 10 μM ranolazine, HIF-1alpha increased in cells exposed to 1000 μM $CoCl_2$ for 24 h, whereas HIF-1alpha decreased in cells exposed to 1000 μM $CoCl_2$ for 48 h. Endothelial cell viability decreased with a high concentration of $CoCl_2$. Ranolazine (1 μM, 10 μM) added to the medium failed to restore cell viability as measured by WST-1. The proportional percentage of cells in which only the MAP kinase pathway was activated increased during chemical hypoxia. Although ranolazine could reduce HIF-1alpha levels in the 48hour group, it had no beneficial effect on $CoCl_2$ toxicity.

Keywords: ranolazine, hypoxia, Human Umbilical Vein Endothelial Cells, *in vitro*

It has been shown that ranolazine has beneficial effects when added to the treatment of symptomatic patients with stable angina pectoris (1, 2). The beneficial effects of ranolazine, especially for treating stable angina pectoris in type 2 diabetes mellitus patients, have been shown in the literature and are included as an adjunct drug in current treatment protocols (3). Ranolazine blocks the late Na^+ current in cardiomyocytes, which prevents the damage caused by Na^+ induced Ca^{+2} overload after ischemia (4). It has also been shown that ranolazine's late Na^+ current blocking effect has vasoactive properties (5). In a clinical study, brachial arteries of patients who received ranolazine for 12 weeks were examined and improvements in flow-mediated relaxation and nitroglycerin-mediated relaxation properties of brachial arteries have been reported (6). It has also been shown that ranolazine may have vasodilator properties through alpha 1receptors on vascular smooth muscle cells (7). Therefore, its vasoactive properties may contribute to the beneficial effect of ranolazine for treating angina pectoris. Also, beneficial effects of ranolazine have been shown in an ischemia-reperfusion model *in vivo* in rabbits (8); pro-inflammatory, anti-inflammatory, and antioxidant effects of ranolazine have been shown in neuron cell culture *in vitro* (9). The effects of ranolazine on endothelial cells have not been investigated in detail in the literature. Therefore, we evaluated the effect of ranolazine on endothelial cell culture under hypoxic stress.

The cobalt chloride-mediated chemical hypoxia model, which is one of the hypoxic cell culture models, has similar properties to the models created by reducing oxygen (10, 11). The substitution of Fe^{+2} by cobalt in the active site of prolyl hydroxylases causes the stabilization of HIF-1α accepted as the key mechanism of the chemical-induced hypoxia model (11). Besides, regulation of HIF-1α stability by nitric oxide (NO) is reported in mammalian cells and the inhibitor role of NO in HIF-1α accumulation during hypoxia was shown (12). The relationship between phosphatidylinositol 3-kinase (PI3K) and mitogen-activated protein kinase (MAPK) pathways with HIF-1α has been shown (13, 14). It has

* Corresponding author: e-mail: edipgcekic@mu.edu.tr

been reported that elevated activities of the PI3K signaling pathway may contribute to the remodeling effects of chemically induced hypoxia (13). It has been reported that increased levels of HIF-1α during acute hypoxia can be inhibited by MAPK/ERK inhibitor and PI3K inhibitor (15). So, this study aimed to investigate the effects of ranolazine on endothelial cells which were exposed to chemical hypoxia with $CoCl_2$, and to demonstrate the roles of HIF-1α, endothelial nitric oxide synthase, and MAPK/PI3K pathways.

EXPERIMENTAL

Cell culture

In this study, the Human Umbilical Vein Endothelial Cells (HUVECs) (CRL-1730; ATCC, Manassas, VA, USA) line was used. Before the procedure, the cryovial of the HUVECs was removed from the -80°C deep freezer. Cells were grown in RPMI-1640 medium (including 10% FBS, 1% pen/streptomycin, 1% amphotericin B) in a 25 cm^2 flask in a 37°C, 5% CO_2 incubator. The cells were passaged with Trypsin/EDTA Solution when they reached approximately 70%-80% confluency.

Experimental groups

$CoCl_2$ (purchased from Sigma) stock solution, which is prepared with ultrapure water to obtain 25 mM, was added to RPMI-1640 medium with a final concentration of 100 µM, 300 µM, and 1000 µM. These different concentrations of $CoCl_2$ were applied for 24 h and 48 h to induce chemical hypoxia. The control group was not exposed to $CoCl_2$. Ranolazine (purchased from Sigma) was tested for chemical hypoxia in HUVECs at two different final concentrations (1 µM and 10 µM). In each 24 h $CoCl_2$ exposure experiment and 48 h $CoCl_2$ exposure experiment 12 groups were planned, as follows:

WST-1 analysis

After the experimental groups were formed cells were planted in 96-well plates, and 10 µL of WST-1 (from BioVision) solution was added to each well and incubated for 2-4 hours at 37°C in the dark. Cell viability was determined by measuring absorbance at 450 nm wavelength in the ELISA plate reader (16). The results of the experiments were calculated as percent viability. Analysis was performed on at least 3 replicates for each group.

Immunocytochemical (ICC) staining

Sterile round coverslips were placed in a 24-well plate where HUVECs were plated as 5 x 103 cells/well and incubated overnight. The wells were washed once with sterile PBS and fixed with 4% paraformaldehyde for 30 min room temperature. After fixation, they were washed thrice with PBS for five minutes. After applying 3% hydrogen peroxide (H_2O_2) solution at room temperature for five minutes, the wells were washed thrice with PBS again. For permeabilization, they were incubated with 0.1% Triton-X 100 at +4°C for 15 min and then washed thrice with PBS. After one hour of blocking solution treatment, cells were incubated at +4°C overnight and anti- HIF-1α and anti-eNOS antibodies were applied at the dilutions recommended by the manufacturer. Then, they were rinsed with PBS and incubated with biotinylated anti-polyvalent for 10 min and streptavidin peroxidase for 10 min at room temperature, respectively. Staining was completed with the chromogen substrate for 15 min, and slides were counterstained with Mayer's hematoxylin for 1 min and rinsed with tap water. Washed coverslips were removed from the 24-well plate and covered with an aqueous mounting medium. Control staining was performed to test whether the immunoreactivities were specific. Experiments were run independently of each other in three parallels.

	Group 1	Group 2	Group 3	Group 4
$CoCl_2$	-	100 µM	300 µM	1000 µM
Ranolazine	-	-	-	-

	Group 5	Group 6	Group 7	Group 8
$CoCl_2$	-	100 µM	300 µM	1000 µM
Ranolazine	1 µM	1 µM	1 µM	1 µM

	Group 9	Group 10	Group 11	Group 12
$CoCl_2$	-	100 µM	300 µM	1000 µM
Ranolazine	10 µM	10 µM	10 µM	10 µM

Evaluation of ICC staining: Immunostained coverslips were evaluated under a light microscope (Nikon Eclipse 80i, Japan). The image obtained at X20 magnification of the antibody-labeled areas on the coverslips was evaluated semiquantitatively using the open source "ImageJ Fiji" software with the method reported in the literature (17, 18).

Analysis of the PI3K/MAPK activity assay

To evaluate the activation state of the PI3K/MAPK pathway in HUVECs the "Muse PI3K/MAPK Dual Pathway activation Kit" was used. The MAPK, PI3K, and dual activation pathways were evaluated after $CoCl_2$ exposure for 48 h. The activated cell percentage distributions were calculated as follows. Cells were resuspended by adding 50 µL of 1X assay buffer (AB) per 100,000 cells. Equal parts (1 : 1) fixation buffer (FB) was added to the cell suspension. A total of 100 µL of cell fixation solution was obtained by adding 50 µL of FB per 50 µL of 1X AB. Incubated for 10 min on ice. The mixture was centrifuged at 300xg for 5 min and the supernatant was discarded. Permeabilization was performed by adding 100 µL of ice-cold 1X Permeabilization Buffer and incubating on ice for 10 min. The mixture was centrifuged at 300 xg for five minutes and the pellet was resuspended with 90 µL 1X AB per 100000 cells. 10 µL of antibody working cocktail solution (5 µL of anti-phospho-Akt Alexa Fluor 555 conjugated antibody and 5µL of anti-phospho-ERK1/2 PECy5 conjugated antibody) was added to each microcentrifuge tube containing the cell suspension. Samples were incubated for 30 min at room temperature in the dark. 100 µL of 1X AB was added to each tube and centrifuged at 300 xg for five minutes. The pellet was resuspended with 200 µL of 1X AB and cells were analyzed with Muse Cell Analyzer and the percentage of cells was estimated by Muse analysis software (19). Experiments were run in triplicate.

Statistical analysis

The obtained data were recorded in the Microsoft Excel (2019) datasheet. GraphPad Prism (trial version 9.1.2 for Windows, San Diego, California, USA) was used for statistical analysis and graph generation. A two-way analysis of variance (Two-way ANOVA) was used to evaluate the data. A p-value of < 0.05 was considered statistically significant.

RESULTS

Cell viability

Chemical hypoxia induced by different $CoCl_2$ concentrations (100 µM, 300 µM, and 1000 µM) in HUVECs for 24 and 48 h caused a significant decrease in cell viability. The highest decrease was observed at the 1000 µM dose of $CoCl_2$ for both 24 and 48 h (Figure 1, Table 1). Different concentrations of ranolazine (1 µM and 10 µM) could not increase the cell viability of HUVECs that were decreased by $CoCl_2$ toxicity (Figure 1, Table 1).

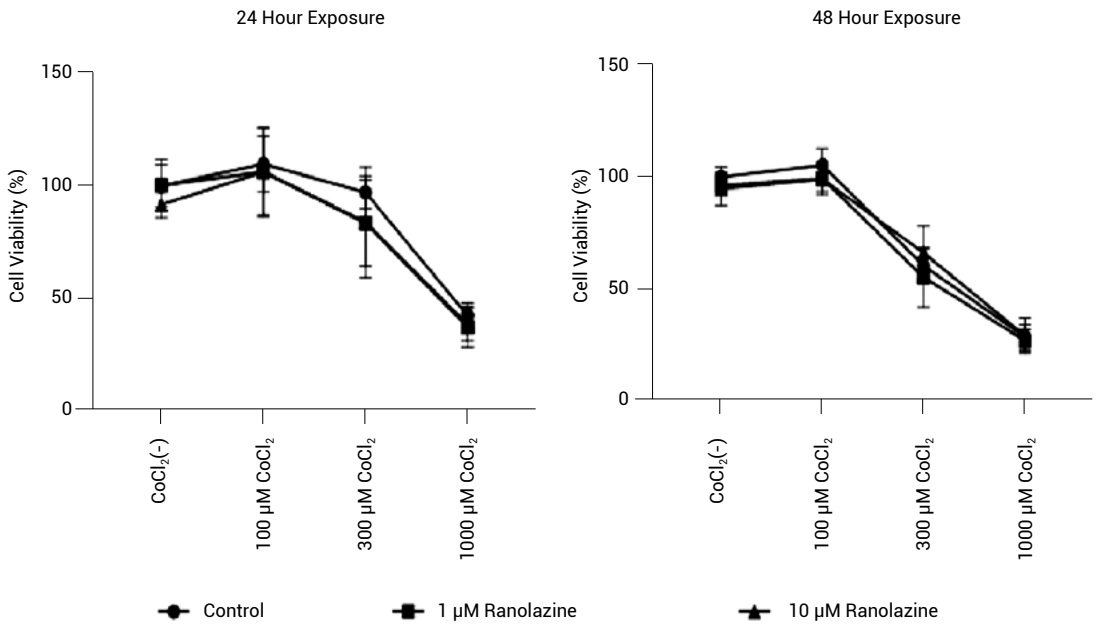

Figure 1. Cell viability of HUVECs after $CoCl_2$ exposure in the presence and absence of ranolazine for 24 h and 48 h

Table 1. Cell viabilities of HUVECs after 24 and 48 hours of $CoCl_2$ exposure

Cell viability after 24 h exposure to $CoCl_2$ in HUVEC cell culture

	Control		Ranolazine (1 μM)		Ranolazine (10 μM)	
	Mean	SD	Mean	SD	Mean	SD
$CoCl_2$ (-)	100.00	9.46	100.35	11.26	91.72	5.78
100 μM $CoCl_2$	109.79	12.32	106.30	19.90	106.29	19.16
300 μM $CoCl_2$	97.15	7.39	83.57	19.15	83.99	24.46
1000 μM $CoCl_2$	42.47	5.35	37.36	8.90	38.41	7.22

Cell viability after 48 h exposure to $CoCl_2$ in HUVEC cell culture

	Control		Ranolazine (1 μM)		Ranolazine (10 μM)	
	Mean	SD	Mean	SD	Mean	SD
$CoCl_2$ (-)	99.99	4.61	96.08	4.73	94.63	7.33
100 μM $CoCl_2$	105.23	7.45	99.18	7.21	98.89	5.41
300 μM $CoCl_2$	60.20	7.77	54.91	13.19	65.89	12.00
1000 μM $CoCl_2$	28.26	5.52	26.65	4.95	28.81	8.02

Cell viability was shown as a percentage

$CoCl_2$: Cobalt chloride

Immunocytochemical evaluation

HIF-1α staining was increased in a time- and dose-dependent manner after $CoCl_2$ exposure (Figures 2 and 3). It was shown that 1 μM ranolazine couldn't decrease HIF-1α levels due to $CoCl_2$ (Figures 2 and 3). The intensity of HIF-1α staining, after the 10 μM ranolazine, increased compared with1000 μM $CoCl_2$ for 24 h ($P < 0.05$), while a significant decrease was observed in 48 h ($P < 0.05$) (Figure 3).

The intensity of eNOS staining was slightly increased in 300 μM and 1000 μM $CoCl_2$ groups after 24 h and 48 h compared with the control group however ranolazine could not affect eNOS levels in a time- and dose-dependent manner (Figures 4 and 5).

Activation of the PI3K/MAPK pathway

MAPK and PI3K, intracellular signaling pathways of endothelial cells exposed to increasing concentrations of cobalt chloride, were examined. Among the evaluated cells, it was shown that the percentage of distribution of only MAPK pathway activated cells increased, while the percentage of cells with only PI3K pathway activated and the percentage of both pathways activated decreased, respectively: 10.25 to 63.21%, 16.22 to 3.68%, and 67.0 to 24.25% (Figure 6).

The proportional distribution of cells showing changes in the activation of their intracellular pathways in the presence of ranolazine (1 μM and 10 μM) is shown in Table 2 and Figure 6.

DISCUSSION

In this study, the model of the HUVEC line exposed to cobalt chloride was used to evaluate the effect of chemicals/drugs that could affect chemical hypoxia. Thus, the effects of ranolazine on hypoxia in endothelial cells could be evaluated. Although ranolazine was shown to decrease HIF-1α levels on HUVECs in which chemical hypoxia was induced for 48 h, no beneficial effect on cell viability was demonstrated.

$CoCl_2$ used to induce chemical hypoxia provides long-term stabilization of HIF-1α and 2α under normoxic conditions (11). It has been shown that the cobalt chloride-induced HIF-1α increase in cell cultures is dose- and time-dependent (11). It is known that HIF-1α is an essential regulatory transcription factor that regulates the hypoxia response (11). It has been shown that hypoxia and increased HIF-1α affect VEGF-mediated angiogenesis and glucose metabolism of endothelial cells (20, 21). Additionally, the NRDG2 gene, which is thought to be associated with hypoxia-mediated apoptosis in tumor cells, has been shown to be regulated by HIF-1α in a hypoxic environment (22). It has been shown that the decrease in cell viability and the increase in HIF-1 alpha levels according to the exposure of cobalt chloride used in our study are consistent with the literature (11, 23). Although it was shown that ranolazine has a viability-enhancing and apoptosis-preventing effect on primary astrocyte culture, such an effect was

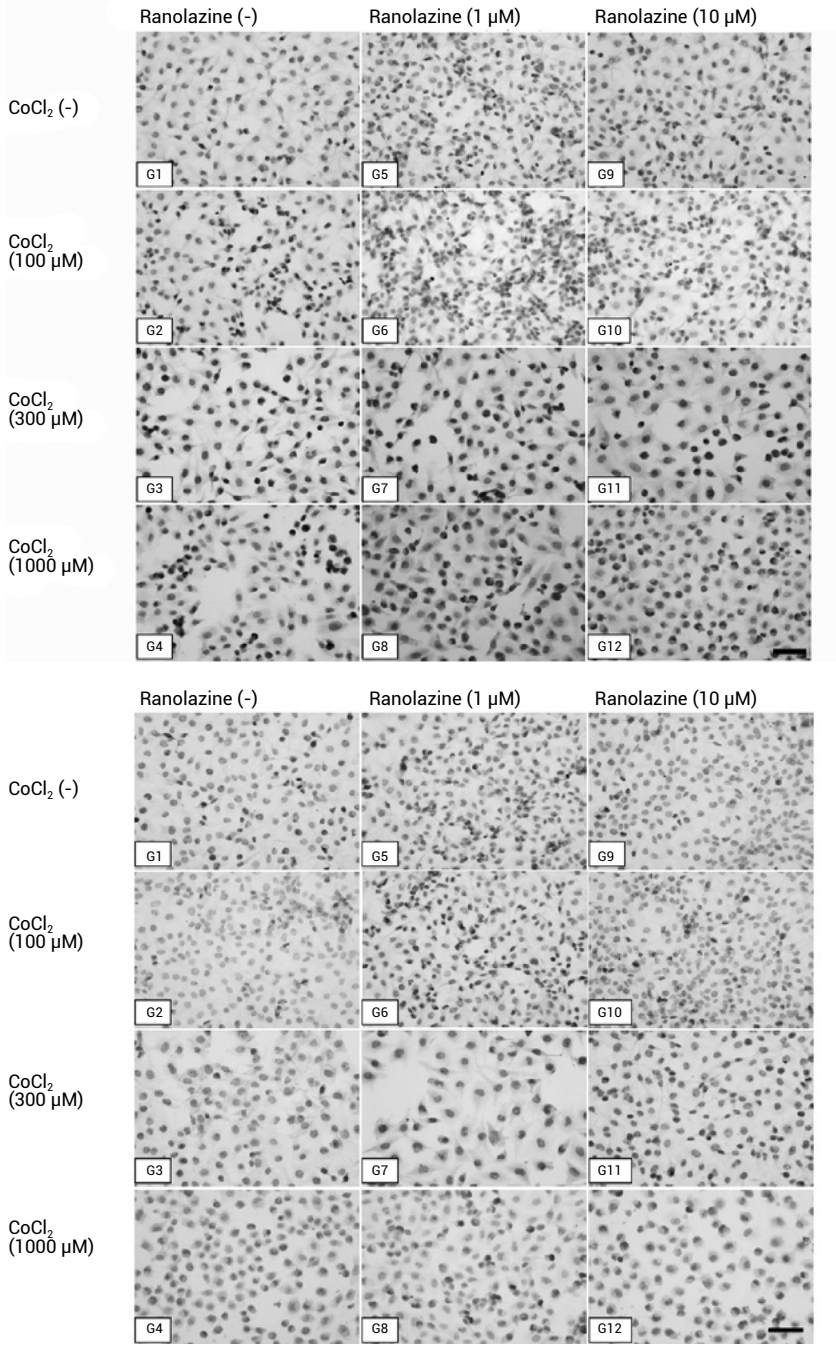

Figure 2. The immunocytochemistry images of HIF-1α in HUVECs for 24 h (a) and 48 h (b). G1: control, G2: 100 µM $CoCl_2$, G3: 300 µM $CoCl_2$, G4: 1000 µM $CoCl_2$, G5: control + 1 µM Ranolazine, G6: 100 µM $CoCl_2$+ 1 µM Ranolazine, G7: 300 µM $CoCl_2$+ 1 µM Ranolazine, G8: 1000 µM $CoCl_2$+ 1 µM Ranolazine, G9: Control + 10 µM Ranolazine, G10: 100 µM $CoCl_2$+ 10 µM Ranolazine, G11: 300 µM $CoCl_2$+ 10 µM Ranolazine, G12: 1000 µM $CoCl_2$+ 10 µM Ranolazine, (x20)

not observed in our study (9). It has been reported that this protective effect on astrocytes may be due to the reduction of the release of pro-inflammatory mediators (IL-1β and TNF-α) through the Na+ channels blocked by ranolazine in microglia cells and the increase in the anti-inflammatory PPAR gamma (9). However, in our study, neither the inhibition of HIF-1α after 48 h of $CoCl_2$ exposure nor the possible Na^+ channel blockage effect of ranolazine in endothelial cells affected decreased viability.

It has been shown that nitric oxide can inhibit the stabilization of HIF-1α during hypoxia (24) and a possible role of HIF-1α in increased nitric oxide production in the cobalt chloride-induced chemical

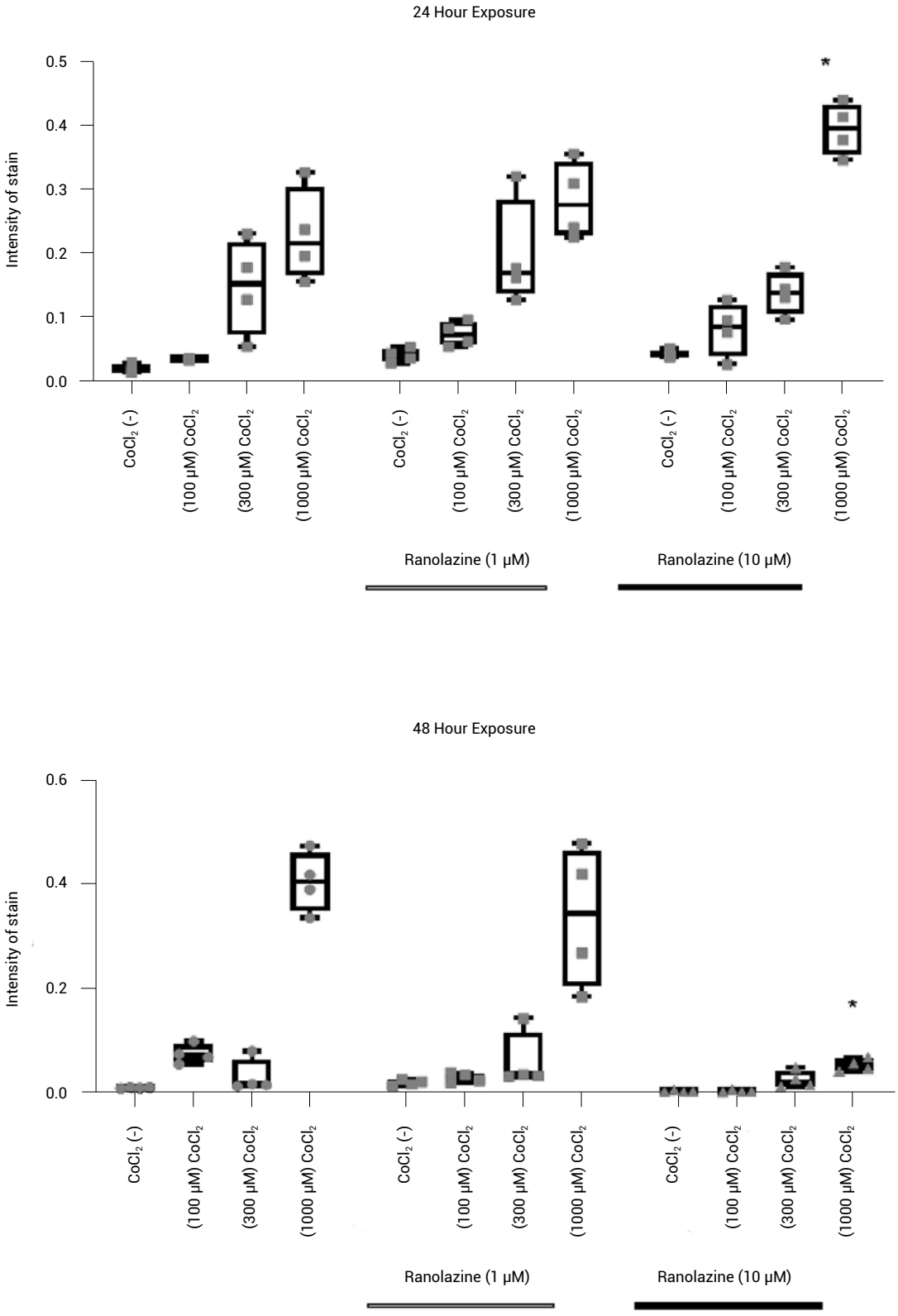

Figure 3. Intensity values (arbitrary unit) of HIF-1α staining in HUVECs after $CoCl_2$ exposure in the presence and absence of ranolazine for 24 h and 48 h. All values (min, max, upper quartile, median, lower quartile) are shown in the whisker and box plot
*P < 0.05 compared to the control group

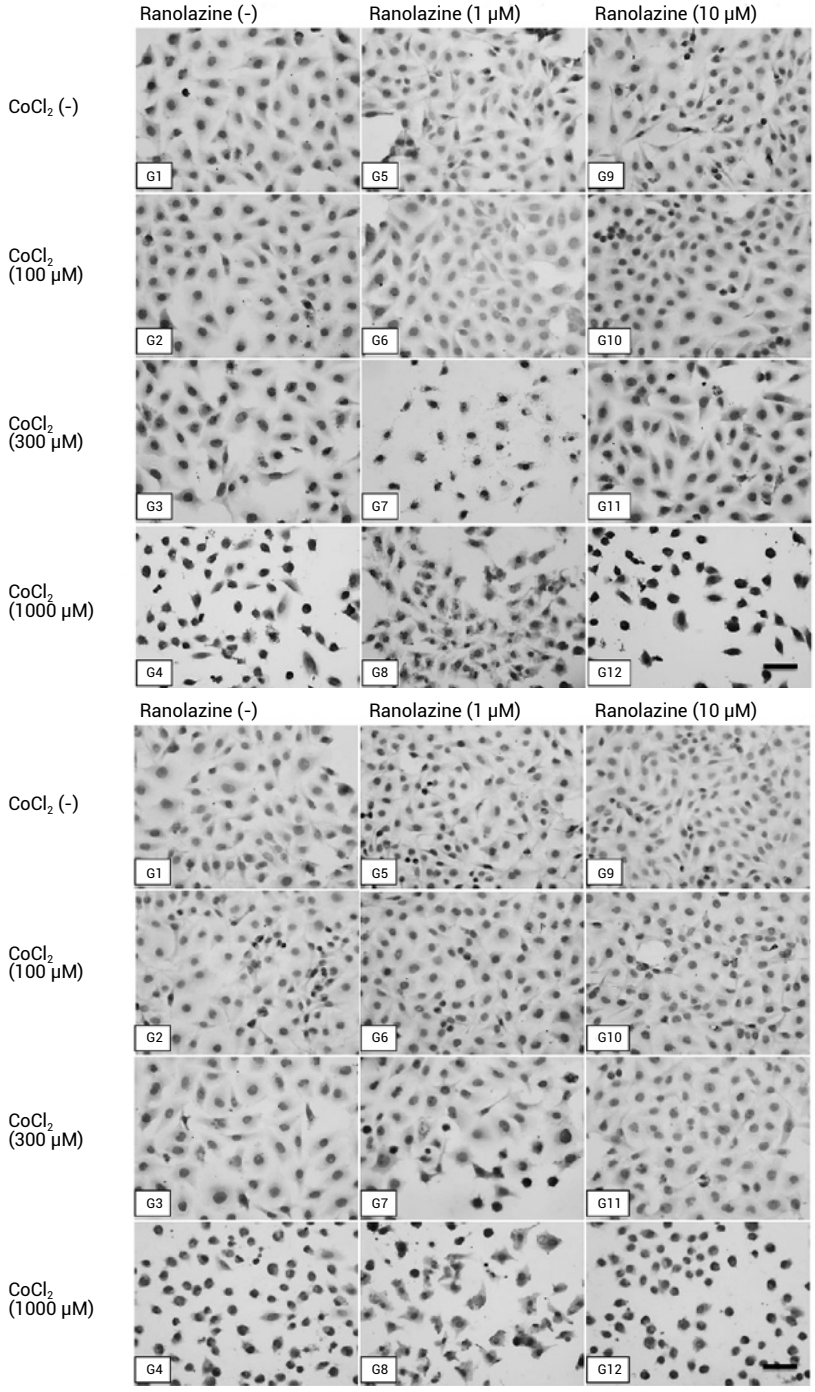

Figure 4. The immunocytochemistry images of eNOS stain in HUVECs for 24 h (a) and 48h (b) exposure to CoCl2. G1: control, G2: 100 μM $CoCl_2$, G3: 300 μM $CoCl_2$, G4: 1000 μM $CoCl_2$, G5: control + 1 μM Ranolazine, G6: 100 μM $CoCl_2$+ 1 μM Ranolazine, G7: 300 μM $CoCl_2$+ 1 μM Ranolazine, G8: 1000 μM $CoCl_2$+ 1 μM Ranolazine, G9: control + 10 μM Ranolazine, G10: 100 μM $CoCl_2$+ 10 μM Ranolazine, G11: 300 μM $CoCl_2$+ 10 μM Ranolazine, G12: 1000 μM $CoCl_2$+ 10 μM Ranolazine, (x20).

hypoxia model in neuronal cells (25). Therefore, it would be interesting to investigate the eNOS activity in the chemical hypoxia model induced by cobalt chloride to further elucidate the complex relationship between nitric oxide and HIF-1α. No significant changes were observed in the groups measured semi-quantitatively using the eNOS antibody during the cobalt chloride-induced chemical hypoxia model. Possibly uninduced eNOS activity against the hypoxic stress response was associated with the inability to achieve a significant cellular response in this model (26, 27). Cellular toxicity caused by

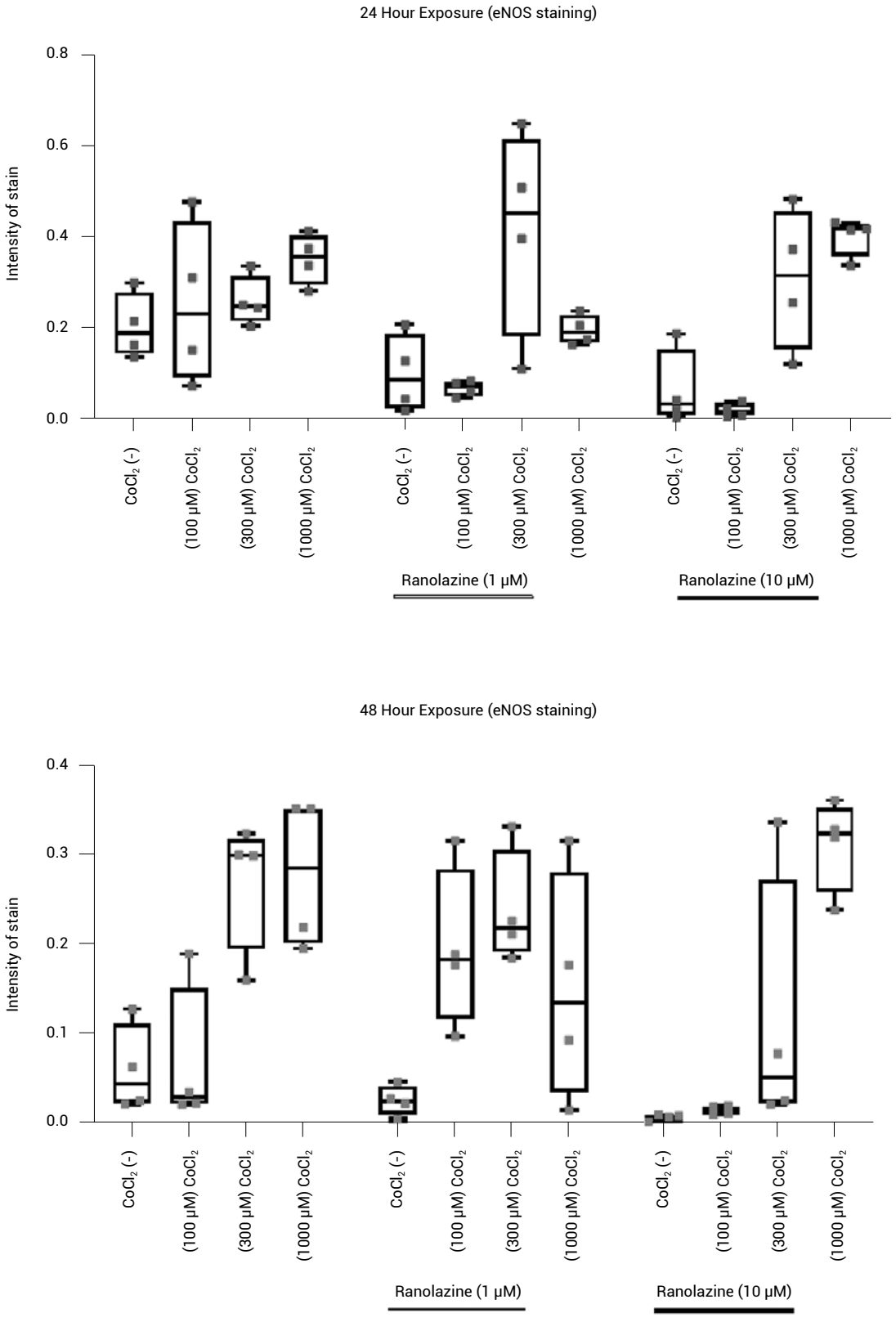

Figure 5. Intensity values (arbitrary unit) of eNOS staining in HUVECs after $CoCl_2$ exposure in the presence and absence of ranolazine for 24 h and 48 h. All values (min, max, upper quartile, median, lower quartile) are shown in the whisker and box plot
*$P < 0.05$ compared to the control group

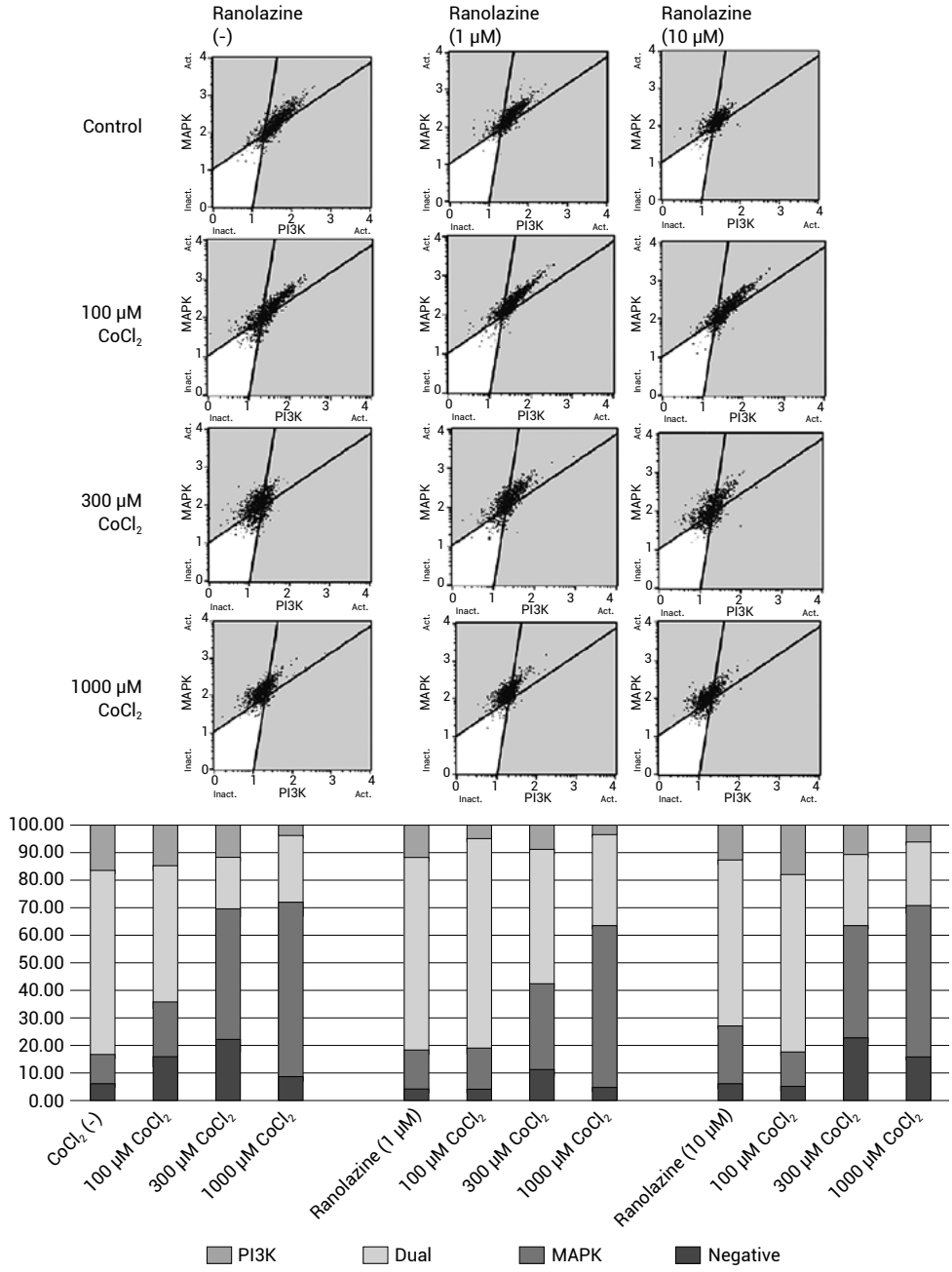

Figure 6. The percentage distribution of MAPK, PI3K and dual activation after $CoCl_2$ exposure in the presence and absence of ranolazine for 48 h

cobalt chloride-mediated hypoxia was thought to be related to the high variability in data.

Mitogen-activated protein kinase (MAPK) and phosphatidylinositol 3 kinase (PI3K) signaling pathways are associated with many cellular activities such as cell viability, proliferation, metabolism, and movement (28, 14). Because of inhibition of MAPK and PI3K pathways with pharmacological agents, a significant decrease in HIF-1α mRNA and protein levels has been detected (15). In our study, we have shown that during chemical hypoxia, the proportional distribution of cells with only MAPK pathway active may increase compared with those with active intracellular pathways. The proportional change in the distribution of cells in which the MAPK and PI3K pathways are activated may be related to the regulation of HIF-1α levels, but further studies must detect a significant relationship and demonstrate the effects of therapeutic agents such as ranolazine on this distribution.

Table 2. Percentage distribution of MAPK. PI3K and dual activation after $CoCl_2$ exposure in the presence and absence of ranolazine for 48h in HUVECs

	Control			
	Negative	MAPK	Dual	PI3K
$CoCl_2$ (-)	6.52	10.25	67.01	16.22
100 µM $CoCl_2$	16.10	19.75	49.56	14.59
300 µM $CoCl_2$	22.38	47.30	18.81	11.51
1000 µM $CoCl_2$	8.87	63.21	24.25	3.68
	Ranolazine (1 µM)			
	Negative	MAPK	Dual	PI3K
$CoCl_2$ (-)	4.39	13.96	70.02	11.62
100 µM $CoCl_2$	4.05	15.06	76.06	4.83
300 µM $CoCl_2$	11.19	31.32	48.74	8.75
1000 µM $CoCl_2$	4.68	58.87	33.11	3.34
	Ranolazine (10 µM)			
	Negative	MAPK	Dual	PI3K
$CoCl_2$ (-)	6.35	20.87	60.19	12.60
100 µM $CoCl_2$	5.34	12.20	64.54	17.92
300 µM $CoCl_2$	22.85	40.72	25.78	10.64
1000 µM $CoCl_2$	15.97	54.79	23.23	6.00

A limitation of the study is that the metabolism of ranolazine, which is extensively metabolized by CYP enzymes, or the effects of ranolazine metabolites on the cell line used, was not evaluated in this study.

CONCLUSIONS

As a result, in the chemical hypoxia model created in endothelial cells, ranolazine could decrease HIF-1α only in the 48-hour group and could not correct the toxic effect of cobalt chloride.

Acknowledgment and funding

This study has been granted by the Mugla Sitki Kocman University Research Projects Coordination Office through Project Grant Number: (19/081/09/3/4).

Conflict of interest

The authors declare no conflicts of interest.

REFERENCES

1. Knuuti J., Wijns W., Saraste A., Capodanno D., Barbato E, et al.: Eur. Heart J. 41, 407 (2020).
2. Chaitman B.R., Pepine C.J., Parker J.O., Skopal J., Chumakova G., et al.: JAMA 291, 309 (2004).
3. Kosiborod M., Arnold S.V., Spertus J.A., McGuire D.K., Li Y., et al.: J. Am. Coll. Cardiol. 61, 2038 (2013).
4. Ambrosio G., Mugelli A., Lopez-Sendón J., Tamargo J., Camm J.: Eur. J. Prev. Cardiol. 23, 1401 (2016).
5. Deng C-Y., Kuang S-J., Rao F., Yang H., Fang X-H., et al.: Eur. J. Pharmacol. 683, 211 (2012).
6. Rehberger-Likozar A., Šebeštjen M.: Coron. Artery Dis. 26, 651 (2015).
7. Virsolvy A., Farah C., Pertuit N., Kong L., Lacampagne A., et al.: Sci. Rep. 5, 17969 (2016).
8. Efentakis P., Andreadou I., Bibli S-I., Vasileiou S., Dagres N., et al.: Eur. J. Pharmacol. 789, 431 (2016).
9. Aldasoro M., Guerra-Ojeda S., Aguirre-Rueda D., Mauricio M.D., Vila J.M., et al.: PloS One 11, e0150619 (2016).
10. Wu D., Yotnda P.: J.Vis. Exp. 54, 2899 (2011).
11. Muñoz-Sánchez J., Chánez-Cárdenas M.E.: J. Appl. Toxicol. 39, 556, (2019).
12. Agani F.H., Puchowicz M., Chavez J.C., Pichiule P., LaManna J.: Am. J. Physiol. Cell Physiol. 283, C178 (2002).
13. Cheng C-I., Lee Y-H., Chen P-H., Lin Y-C., Chou M-H., et al.: Cell. Signal. 36, 25 (2017).

14. Zhang Z., Yao L., Yang J., Wang Z., Du G.: Mol. Med. Rep. 18, 3547 (2018).
15. Zhang Q., Cui B., Li H., Li P., Hong L., et al.: Biochem. Biophys. Res. Commun. 438, 507 (2013).
16. Tu D-G., Yu Y., Lee C-H., Kuo Y-L., Lu Y-C., et al.: Oncol. Lett. 11, 2934 (2016).
17. Schindelin J., Arganda-Carreras I., Frise E., Kaynig V., Longair M., et al.: Nat. Methods 9, 676 (2012).
18. Crowe A.R., Yue W.: Bio Protoc. 9, e3465 (2019).
19. Krutzik P.O., Nolan G.P.: Cytometry A. 55, 61 (2003).
20. Majmundar A.J., Wong W.J., Simon M.C.: Mol. Cell 40, 294 (2010).
21. Tang N., Wang L., Esko J., Giordano F.J., Huang Y., et al.: Cancer Cell 6, 485 (2004).
22. Wang L., Liu N., Yao L., Li F., Zhang J., et al.: Cell. Physiol. Biochem. 21, 239 (2008).
23. Mo S-J., Hong J., Chen X., Han F., Ni Y., et al.: Neurosci. Lett. 610, 54 (2016).
24. Hagen T., Taylor C.T., Lam F., Moncada S.: Science 302, 1975 (2003).
25. Li G., Zhao Y., Li Y., Lu J.: NeuroMolecular Med. 17, 443 (2015).
26. Forstermann U., Sessa W.C.: Eur. Heart J. 33, 829 (2012).
27. Gunnett C.A., Lund D.D., McDowell A.K., Faraci F.M., Heistad D.D.: Arterioscler. Thromb. Vasc. Biol. 25, 1617 (2005).
28. Guo Y., Pan W., Liu S., Shen Z., Xu Y., et al.: Exp. Ther. Med. 19, 1997 (2020).